# GAS PHASE REACTIONS OF S-BUTANETHIOL WITH SELECTED METAL IONS

**John (Hanna) El-Nakat, Noha Ghanem, Keith Fisher[1] and Gary Willet[1]**
University of Balamand, P.O. Box 100, Tripoli, Lebanon
[1] University of New South Wales, P.O. Box 1, Kensington, NSW 2033, Australia
john.nakat@balamand.edu.lb

(Received 7 July 2010 - Accepted 18 February 2011)

***ABSTRACT***

*A gas phase ion molecule reaction study of s-butanethiol with selected metal ions ($Ag^+$, $Cu^+$, $Cd^+$, $Pb^+$, $Zn^+$, $Cr^+$, $Mn^+$, $Ni^+$, $Fe^+$, $Co^+$, $Pt^+$ and $Au^+$) using mass spectrometry is described. The reaction pathways and, consequently, the reaction mechanisms were proposed by observing the variation of the normalized intensities of the different ions with time. The reactivity of $Bu^s$-SH with respect to the selected metal ions was studied in terms of the time needed for the complete disappearance of the metal ion, the variety of products obtained and the number of reaction pathways proposed.*

**Keywords:** FT- ICR/MS, gas phase chemistry, progress of the reactions, reaction pathways, secondary butanethiol, metal-ligand complex mono-cations

## INTRODUCTION

The gas phase ions molecule reactions of transition metal ions with organic molecules is a well established area of mass spectrometry. The first observation of metal-ion activation of saturated organic compounds was made by Allison *et al*. (1979). Eller and Schwarz (1990; 1991) referred to 700 publications on organometallic gas phase ion chemistry from the literature covered up to early 1991.

This stimulus for the study of organometallic molecules lies in both the theoretical and the industrial application of such reactions. Besides, gas phase reaction can provide insight into the ligand binding energies, reaction pathways, and the kinetics and thermodynamic consequences of such reactions.

The ability to physically isolate gas phase metal ions which are free from the influences of the ligand and of the solvent, as well as free from ion-pairing, offers a unique opportunity to probe the inherent characteristic properties of a particular metal ion or complex and/or the properties of an organic molecule. The use of a pulsed neodynium-doped yttrium aluminum garnet (Nd-YAG) laser on a Fourier Transform Mass Spectrometer has proved to be a convenient and powerful method of generating bare metal ions for subsequent gas phase studies (El-Nakat *et al*., 1992; 1994).

Gas phase chemistry remains an attractive field for research. In the year 2001, Fisher (2001) has dedicated a whole chapter discussing the theory of gas phase chemistry and summarizing its different applications. Recent literature is still rich with publications on ion-

molecule gas phase reactions (Zhang *et al*., 2005; Lennon *et al*., 2006; Xia *et al*., 2006; Choi & So, 2006; Kumar, Prabahakar *et al*., 2006; Kumar, Sateesh *et al*., 2006; Olesik & Jones, 2006), yet there are still a lot of unexplored areas in this field. "To me it appears like a primeval tropical forest full of the most remarkable things, a dreadful endless jungle into which one does not dare enter for there seems to be no way out" – Friedrich Wohler, 1835.

In this study the use of very small time intervals has allowed the observation of new product ions. Accordingly, new steps have been proposed in the mechanism normally adopted in metal-ligand gas phase chemistry.

## EXPERIMENTAL

Mass spectra were obtained using a Spectrospin CMS-47 (FT-ICR) mass spectrometer, equipped with a 4.7T superconducting magnet (Grenwood *et al*., 1990).

The metal was secured to a satellite probe tip and introduced into the ICR cell using a direct insertion probe. A cylindrical ICR cell (radius 30 x 60 mm) with six titanium single section plates was used in an ultra high vacuum chamber maintained at a base pressure of $10^{-9}$ mbar by a turbomolecular pump (Nguyen *et al*., 1991).

Laser-ablation was performed using an Nd-YAG laser (1064 nm, Spectra Physics DCR-11) focused to an area of 0.1 $mm^2$ of the metal target at the end of the cell, flush and in contact with the ICR trapping plate. The laser was used in Q-switched mode producing an 8 ns pulse with a pulse energy being modified by neutral filters (El- Nakat *et al*., 1991).

Positive ions were trapped in the cell by a potential of +4V. A typical pulse sequence is shown in Fig. 1. All ions were removed using an ejection pulse (P2) and a delay (D2) of at least 100 ms was introduced to allow collisional cooling of the metal ions before ion selection (P3) and measurement of the reaction during the period (D3). The data on relative intensities of ions, included in the plots and the kinetic analyses, were obtained by normalization to the sum of the observed ions.

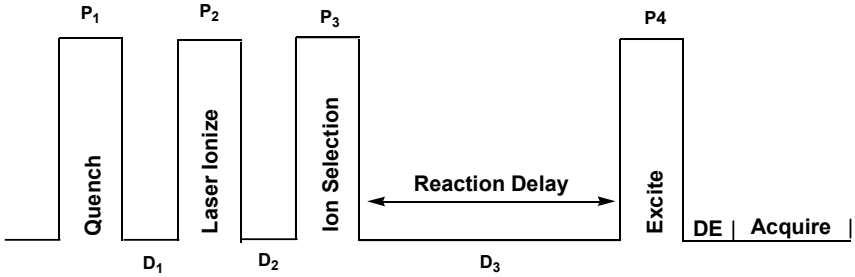


**Figure 1. Typical gas phase ion molecule reaction pulse sequence.**

The reactants were degassed by repeated freeze-thawing and introduced through a heated inlet system (Greenwood *et al*., 1990) to give an uncorrected background pressure of 6.5 x $10^{-8}$ mbar. Ablation was performed in the presence of the reactants.

## RESULTS

Table 1 is a summary of the principle reactions commonly observed for gas phase ion molecule chemistry (eqs 1-6) (El-Nakat *et al*., 1992) which are, as well, observed for this study. Aside from these common pathways, the reactions of the different metal ions with s-butanethiol showed a variety of results, in terms of the products observed, the type of reaction pathways followed (Table 2) and the reaction times required for the total disappearance of the metal ion (Table 3).

**TABLE 1**

**Summary of Principle Gas-Phase Reactions**

| Type of Reaction | Chemical Equation | Eq |
|---|---|---|
| Mono-complex formation: | $M^+ + L \longrightarrow ML^+$ | 1 |
| Bis-complex formation | $ML^+ + L \longrightarrow ML_2^+$ | 2 |
| Charge transfer | $M^+ + L \longrightarrow M + L^+$ | 3 |
| Elimination of $H_2S$ | $M^+ + HSXH \longrightarrow MX^+ + H_2S$ | 4 |
| Elimination of HS | $M^+ + HSXH \longrightarrow MHX^+ + HS$ | 5 |
| Elimination of X | $M^+ + HSXH \longrightarrow MH_2S^+ + X$ | 6 |

There is a continuous reference in the text to L = $HSC_4H_9$ = $Bu^s$ -SH = HSR = HSXH, R = $C_4H_9$, X = $C_4H_8$ and E = $C_4H_6$. In addition, unless specified, ions are classified as:

Major or strong (s) if their normalized relative intensities are greater than 20%
Medium (m) if their normalized relative intensities are between 5% and 20%
Minor or weak (w) if their normalized relative intensities are less than 4%

All species present in Figs 2-10 are the mono-cations produced which are, consequently, detected by the mass spectrometer.

Identical pathway sequences observed for the reactions of the different metal mono-cations are indicated by identical arrows throughout Figs 2-10.

### Reactions of $Ag^+_{(g)}$ and $Cu^+_{(g)}$ with $Bu^s$-SH

The reactions of $Ag^+$ and $Cu^+$ with $Bu^s$-SH reveals, at short time intervals (between 0-2.5 seconds), the presence of the ion species $M(H_2S)^+$ (eq. 6) and $MX^+$ (eq. 4) with medium relative normalized intensities (around 15%). These two ions were observed, independently, to undergo further reactions with neutral molecules of the s-butanethiol to give the mono-complex, $ML^+$ (following eq. 7 & eq. 8), as a major product with maximum normalized

intensity of 60% at about 1.5-2 seconds. Eventually, $ML^+$ gave the bis-complex ion, $ML_2^+$ (eq. 2) and the proton transfer product, $HL^+$ (eq. 9), which was only observed as a minor ion at longer times with relative intensities of the order of up to 4%. The variation of the intensities of the different ions with respect to time has been studied and the mechanism for the reactions was proposed as shown in Fig. 2.

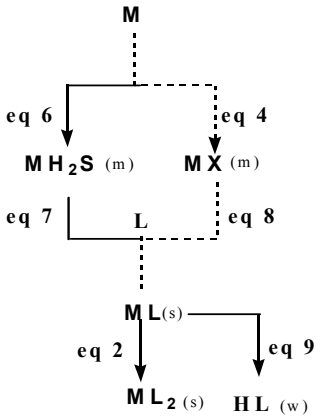


**Figure 2. Mechanistic pathways for the formation of products in the reactions of $Ag^+$ and $Cu^+$ with $Bu^s$ –SH.**

Two points that can be made regarding the reactions of $Cu^+$ and $Ag^+$ with $Bu^s$ -SH are:

The maximum amount of $ML^+$ formation is greater for silver than for copper, but occurs at about 1.5-2 seconds.

The reactions of $Ag^+$ and $Cu^+$ started almost immediately (formation of $M(H_2S)^+$ and $MX^+$ was observed between 0 and 2.5 seconds), but the time for complete disappearance of $Ag^+$ was 3 seconds in comparison to 5 seconds for $Cu^+$.

**Reactions of $Cd^+$ (g) with $Bu^s$-SH**

The reaction of $Cd^+$ with $Bu^s$ -SH was relatively slow and a time interval of 10 seconds was required for the complete disappearance of the $Cd^+$ ion. $CdX^+$ was exhibited as the primary ion which was formed by the elimination of $H_2S$ molecule (eq. 4). Following the change in the normalized intensity of the ions with time, $CdX^+$ was found to reach a maximum of approximately 15 % after a reaction time of 1.5 seconds then disappear by undergoing further reactions with the s- butanethiol molecules to form the mono-complex ion, $CdL^+$, (eq. 8) as a major ion (78%) and the proton transfer ion, $HL^+$, (eq. 10) as a minor ion (intensity < 3%) (Fig. 3).

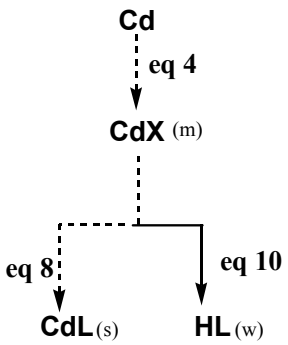


**Figure 3. Mechanistic pathways for the formation of products in the reactions of $Cd^+$ with $Bu^s$ –SH.**

**Reactions of $Pb^+$ (g) with $Bu^s$-SH**

The reactions of the lead ions are characterized by their low reactivity, low variety of products and the long time required for the initiation of the reaction ($Pb^+$ was the only ion detected up to 20 seconds). Approximately 69% of $Pb^+$ reacted after 150 seconds to form the mono-complex $PbL^+$ (45% at 150 seconds) (eq. 1) and $PbSC_2H_4^+$ (24% at 150 seconds) (eq. 11). $PbSC_2H_4^+$ was observed to appear after 50 seconds at a normalized intensity of 6% and then increased in abundance until it reached 23.2% after 150 seconds reaction time. A low intensity proton transfer ion product, $HL^+$, was also detected and it increased to a maximum of 5% at 30 seconds and disappeared after a reaction time of 100 seconds when it was last observed with an intensity of 2% (eq. 12). Following the variation of the normalized intensities of these ions with time, none of the ions was involved in further reactions and that they were all produced from the direct reaction of the lead mono-cation with the neutral molecules of s- butanethiol as indicated.

**Reactions of $Zn^+$ (g) with $Bu^s$-SH**

Fig. 4 represents the normalized intensity distribution of the different ions observed for the reaction of $Zn^+$ with $Bu^s$-SH in relation to time. The primary ion obtained for the reaction was $ZnX^+$ (eq. 4) which reached a maximum of approximately 38% after a reaction time of almost one second and then disappeared as it reacted with the molecules of the s-butanethiol to produce the mono-complex ion (eq. 8) and the proton transfer ion, $HL^+$ (eq. 10). $HL^+$ was observed to increase in intensity until it reached a constant proportion of 18.6% of the total ions. The mono-complex, $ZnL^+$, was observed to maximise at 48% around 3 s after which time it was consumed by further reacting with neutral molecules of s-butanethiol to give the two products $ZnSL^+$ (eq. 13) and $ZnSRL^+$ (eq. 14). $ZnSL^+$ mono-cation was believed to undergo a further addition reaction with a neutral molecule of s-butanethiol to form $ZnSL_2^+$ (eq. 15). Following the same mechanism (addition), $ZnSRL^+$ mono-cation reacted to give $ZnSRL_2^+$ (eq. 16). The mechanistic pathways for the reactions of s-butanethiol with $Zn^+$ are shown in Fig. 5.

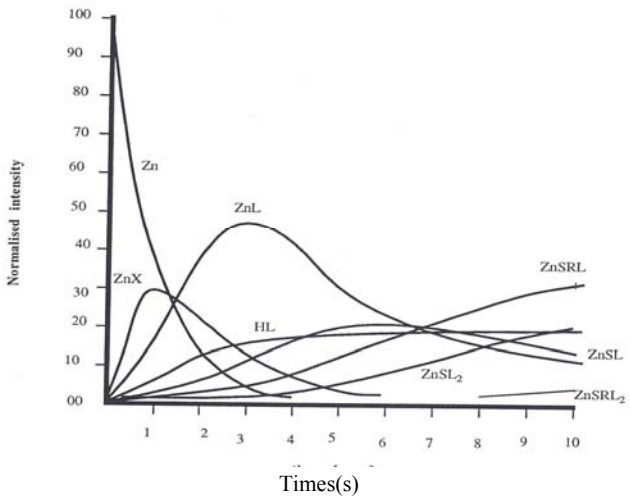


**Figure 4. The intensity distribution for the different ions in the reactions of $Zn^{+}$ with $Bu^{s}$ –SH.**

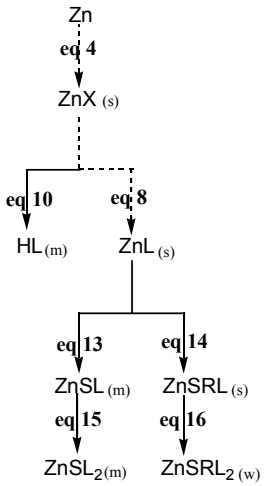


**Figure 5. Mechanistic pathways for the formation of products in the reactions of $Zn^{+}$ with $Bu^{s}$ –SH.**

***Reactions of $Cr^+$ (g) and $Mn^+$ (g) with $Bu^s$-SH***

The reactions of chromium and manganese with $Bu^s$-SH showed a number of similarities with respect to the major ions observed and the reaction pathways followed (Figs 6, 7).

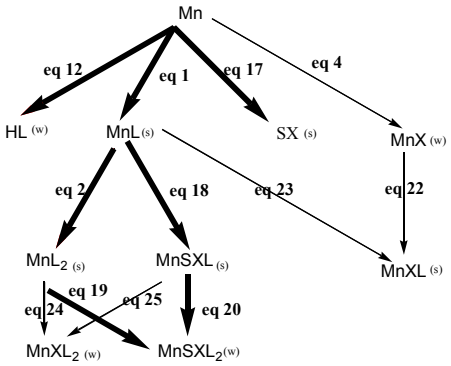


**Figure 6. Mechanistic pathways for the formation of products in the reactions of $Mn^+$ with $Bu^s$ –SH.**

Both metal-ions exhibited the formation of the $SX^+$ ion as a significant product (>10%) (eq. 17) and the proton transfer, $HL^+$, ion as a weak product (≤ 4%) (eq. 12). Another similarity is observed in the formation of the mono complex ion $ML^+$ (eq. 1) which further reacted to give the bis complex $ML_2^+$ (eq. 2) and $MSXL^+$ (eq. 18). The latter two ions were believed to undergo further independent minor reactions to produce $MSXL_2^+$ (eqs 19, 20).

Nevertheless, different reactions and products were also observed for each ion: Although the $MX^+$ ion was observed as a ***weak*** product for both ions (eq. 4), however, $CrX^+$ ion was a minor contributor for the formation of $CrSX^+$ (eq. 21), while $MnX^+$ ion was believed to contribute to the formation of $MnXL^+$ (eq. 22). $MXL^+$ was not observed for $Cr^+$ ion and $MSX^+$ was not observed for $Mn^+$ ion.

Taking into consideration the normalized intensities of $MnX^+$ (w), $MnL^+$ (s) and $MnXL^+$ (s); $MnL^+$ was believed to be the major contributor for the formation of $MnXL^+$ (eq. 23).

For $Mn^+$ ion, $ML_2^+$ and $MSXL^+$ were observed to undergo further, independent, weak reactions to form the $MnXL_2^+$ product (eqs 24 and 25). This $MXL_2^+$ product was not observed for $Cr^+$ ion.

The $MSX^+$ ion was observed only for the reactions of $Cr^+$ ion resulting from the elimination of one hydrogen molecule (eq. 26). $MSX^+$ ion further reacted with molecules of s-butanethiol to give the three products: $CrSX_2^+$ (w) (eq. 27), $Cr(SX)_2^+$ (m) (eq. 28) and $CrSXL^+$ (m) (eq. 29).

$CrL^+$ ion was also believed to contribute to the formation of $Cr(SX)_2^+$ ion by the elimination of two hydrogen molecules (eq. 30).

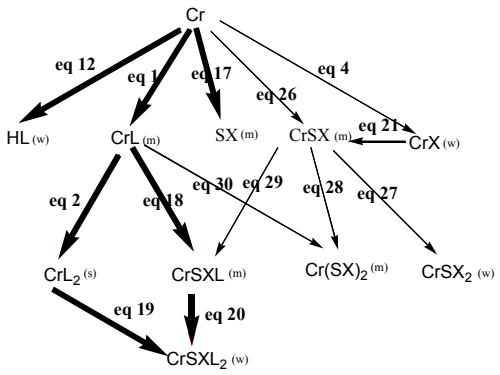


**Figure 7. Mechanistic pathways for the formation of products in the reactions of $Cr^+$ with $Bu^s$ –SH.**

The reactions for both ions started almost immediately. However, the time for complete disappearance of $Cr^+$ ion is five seconds while eight seconds were required for the disappearance of $Mn^+$. At 5 seconds reaction time the normalized intensity for $Mn^+$ was about 15%.

**Reactions of $Ni^+$ (g), $Fe^+$ (g) and $Co^+$ (g) with $Bu^s$-SH**

The reaction of $Bu^s$-SH with $Ni^+$ (g), $Fe^+$ (g) and $Co^+$ (g) were far more complicated. The mechanisms for the formation of the products showed 22 reaction pathways for $Ni^+$, 25 reaction pathways for $Fe^+$ and 21 reaction pathways for $Co^+$ as summarized in Figs 8, 9 and 10 respectively. Although many ions were observed in common, the study of the change in normalized intensities *versus* time revealed that the formation of such ions followed different pathways.

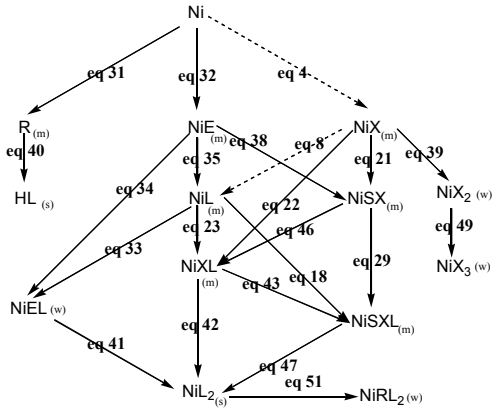


**Figure 8. Mechanistic pathways for the formation of products in the reactions of $Ni^+$ with $Bu^s$ –SH.**

**TABLE 2.1**

**Summary of the Reactions Proposed in this Study**

| Chemical Equation | Eq |
|---|---|
| $M(H_2S)^+ + HSXH \longrightarrow ML^+ + H_2S$ | 7 |
| $MX^+ + HSXH \longrightarrow ML^+ + X$ | 8 |
| $ML^+ + HSXH \longrightarrow HL^+ + MSXH$ | 9 |
| $MX^+ + HSXH \longrightarrow HL^+ + MEH$ | 10 |
| $M^+ + HSXH \longrightarrow MSC_2H_4^+ + C_2H_6$ | 11 |
| $M^+ + 2(HSXH) \longrightarrow HL^+ + MSXH$ | 12 |
| $ML^+ + HSXH \longrightarrow MSL^+ + H_2X$ | 13 |
| $ML^+ + HSXH \longrightarrow MSRL^+ + H^{\cdot}$ | 14 |
| $MSL^+ + HSXH \longrightarrow MSL_2^+$ | 15 |
| $MSRL^+ + HSXH \longrightarrow MSRL_2^+$ | 16 |
| $M^+ + HSXH \longrightarrow SX^+ + M + H_2$ | 17 |
| $ML^+ + HSXH \longrightarrow MSXL^+ + H_2$ | 18 |
| $ML_2^+ + HSXH \longrightarrow MSXL_2^+ + H_2$ | 19 |
| $MSXL^+ + HSXH \longrightarrow MSXL_2^+$ | 20 |
| $MX^+ + HSXH \longrightarrow MSX^+ + H_2X$ | 21 |
| $MX^+ + HSXH \longrightarrow MXL^+$ | 22 |
| $ML^+ + HSXH \longrightarrow MXL^+ + H_2S$ | 23 |
| $ML_2^+ + HSXH \longrightarrow MXL_2^+ + H_2S$ | 24 |
| $MSXL^+ + HSXH \longrightarrow MXL_2^+ + S$ | 25 |
| $M^+ + HSXH \longrightarrow MSX^+ + H_2$ | 26 |
| $MSX^+ + HSXH \longrightarrow MSX_2^+ + H_2S$ | 27 |
| $MSX^+ + HSXH \longrightarrow M(SX)_2^+ + H_2$ | 28 |
| $MSX^+ + HSXH \longrightarrow MSXL^+$ | 29 |
| $ML^+ + HSXH \longrightarrow M(SX)_2^+ + 2H_2$ | 30 |

A total of 48 different reactions were observed for the reactions of $Ni^+$, $Fe^+$ and $Co^+$ with $Bu^s$-SH (Table 2: 2.2 & 2.3). Nevertheless, regardless of the difference in the reactant and product ions, the majority of these reactions take place by a specific type of mechanism pathways:

| | | |
|---|---|---|
| Elimination of $H_2S$ & $H_2$ | 5 reactions | eqs: 32, 33, 36, 48, 59 |
| Elimination of $H_2S$ | 8 reactions | eqs: 4, 23, 24, 37, 39, 49, 54, 62 |
| Elimination of $H_2$ | 3 reactions | eqs: 18, 19, 26 |
| Elimination of E | 5 reactions | eqs: 35, 41, 57, 61, 66 |
| Elimination of X | 7 reactions | eqs: 8, 38, 40, 42, 56, 58, 60 |
| Elimination of $H_2X$ | 3 reactions | eqs: 21, 43, 50 |
| Elimination of S | 3 reactions | eqs: 25, 46, 64 |
| Addition | 6 reactions | eqs: 20, 22, 29, 34, 53, 55 |

Time wise, the reactions of $Ni^+$ (g), $Fe^+$ (g) and $Co^+$ (g) with $Bu^s$-SH showed similar reactivities. All reactions started almost immediately and a reaction time of 5 seconds was sufficient for the complete disappearance of the three metal mono-cations.

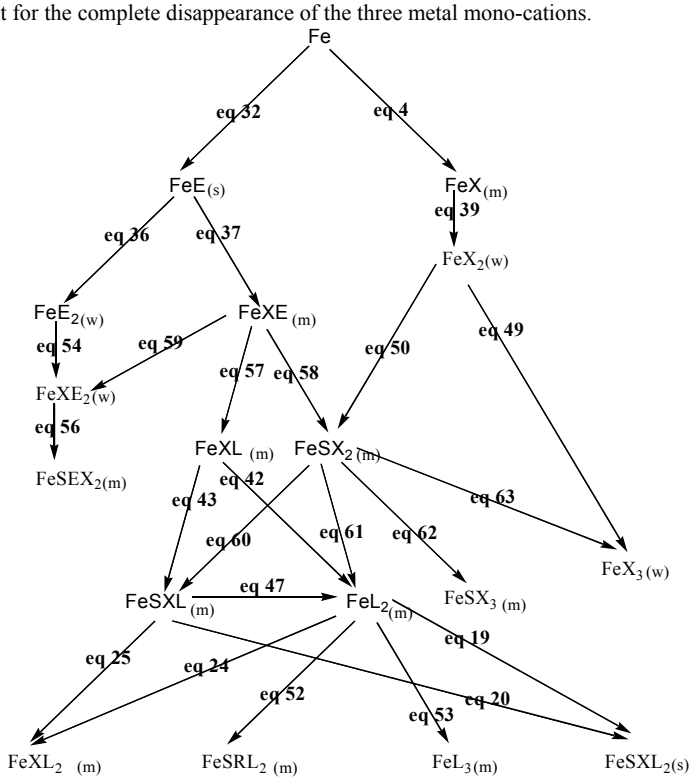


**Figure 9. Mechanistic pathways for the formation of products in the reactions of $Fe^+$ with $Bu^s$ –SH.**

**TABLE 2.2**

**Summary of the Reactions Proposed in this Study**

| $M^+$ mono-cation | Chemical Equation | Eq |
|---|---|---|
| Ni | $M^+ + HSXH \longrightarrow R^+ + MSH$ | 31 |
| Ni, Fe, Co | $M^+ + HSXH \longrightarrow ME^+ + H_2S + H_2$ | 32 |
| Ni, Fe | $M^+ + HSXH \longrightarrow MX^+ + H_2S$ | 4 |
| Co | $M^+ + HSXH \longrightarrow MSX^+ + H_2$ | 26 |
| Ni | $ML^+ + HSXH \longrightarrow MEL^+ + H_2S + H_2$ | 33 |
| Ni | $ML^+ + HSXH \longrightarrow MSXL^+ + H_2$ | 18 |
| Ni | $ML^+ + HSXH \longrightarrow MXL^+ + H_2S$ | 23 |
| Ni | $ME^+ + HSXH \longrightarrow MEL^+$ | 34 |
| Ni | $ME^+ + HSXH \longrightarrow ML^+ + E$ | 35 |
| Fe, Co | $ME^+ + HSXH \longrightarrow ME_2^+ + H_2S + H_2$ | 36 |
| Fe, Co | $ME^+ + HSXH \longrightarrow MXE^+ + H_2S$ | 37 |
| Ni | $ME^+ + HSXH \longrightarrow MSX^+ + X$ | 38 |
| Ni | $MX^+ + HSXH \longrightarrow ML^+ + X$ | 8 |
| Ni | $MX^+ + HSXH \longrightarrow MXL^+$ | 22 |
| Ni | $MX^+ + HSXH \longrightarrow MSX^+ + H_2X$ | 21 |
| Ni, Fe | $MX^+ + HSXH \longrightarrow MX_2^+ + H_2S$ | 39 |
| Ni | $R^+ + HSXH \longrightarrow HL^+ + X$ | 40 |
| Ni | $MEL^+ + HSXH \longrightarrow ML_2^+ + E$ | 41 |
| Ni, Fe, Co | $MXL^+ + HSXH \longrightarrow ML_2^+ + X$ | 42 |
| Ni, Fe, Co | $MXL^+ + HSXH \longrightarrow MSXL^+ + H_2X$ | 43 |
| Co | $MXL^+ + HSXH \longrightarrow MSL^+ + H_2X_2$ | 44 |
| Co | $MXL^+ + HSXH \longrightarrow MSX_2^+ + H_2 + L$ | 45 |
| Ni | $MSX^+ + HSXH \longrightarrow MSXL^+$ | 29 |
| Ni, Co | $MSX^+ + HSXH \longrightarrow MXL^+ + S$ | 46 |

**TABLE 2.3**

**Summary of the Reactions Proposed in this Study**

| $M^+$ mono-cation | Chemical Equation | Eq |
|---|---|---|
| Ni, Fe, Co | $MSXL^+ + HSXH \longrightarrow ML_2^+ + SX$ | 47 |
| Fe | $MSXL^+ + HSXH \longrightarrow MXL_2^+ + S$ | 25 |
| Fe | $MSXL^+ + HSXH \longrightarrow MSXL_2^+$ | 20 |
| Co | $MSXL^+ + HSXH \longrightarrow MSXEL^+ + H_2S + H_2$ | 48 |
| Ni, Fe | $MX_2^+ + HSXH \longrightarrow MX_3^+ + H_2S$ | 49 |
| Fe | $MX_2^+ + HSXH \longrightarrow MSX_2^+ + H_2X$ | 50 |
| Ni | $ML_2^+ + HSXH \longrightarrow MRL_2^+ + HS$ | 51 |
| Fe | $ML_2^+ + HSXH \longrightarrow MXL_2^+ + H_2S$ | 24 |
| Fe | $ML_2^+ + HSXH \longrightarrow MSRL_2^+ + H^{\bullet}$ | 52 |
| Fe | $ML_2^+ + HSXH \longrightarrow ML_3^+$ | 53 |
| Fe | $ML_2^+ + HSXH \longrightarrow MSXL_2^+ + H_2$ | 19 |
| Fe, Co | $ME_2^+ + HSXH \longrightarrow MXE_2^+ + H_2S$ | 54 |
| Co | $ME_2^+ + HSXH \longrightarrow MLE_2^+$ | 55 |
| Fe | $MXE_2^+ + HSXH \longrightarrow MSEX_2^+ + X$ | 56 |
| Fe, Co | $MXE^+ + HSXH \longrightarrow MXL^+ + E$ | 57 |
| Fe, Co | $MXE^+ + HSXH \longrightarrow MSX_2^+ + X$ | 58 |
| Fe, Co | $MXE^+ + HSXH \longrightarrow MXE_2^+ + H_2S + H_2$ | 59 |
| Fe, Co | $MSX_2^+ + HSXH \longrightarrow MSXL^+ + X$ | 60 |
| Fe | $MSX_2^+ + HSXH \longrightarrow ML_2^+ + E$ | 61 |
| Fe | $MSX_2^+ + HSXH \longrightarrow MSX_3^+ + H_2S$ | 62 |
| Fe, Co | $MSX_2^+ + HSXH \longrightarrow MX_3^+ + H_2S_2$ | 63 |
| Co | $MSL^+ + HSXH \longrightarrow ML_2^+ + S$ | 64 |
| Co | $MSXEL^+ + HSXH \longrightarrow ML_2^+ + SXE$ | 65 |
| Co | $MXE_2^+ + HSXH \longrightarrow MEXL^+ + E$ | 66 |

**Reactions of $Au^+$ (g) and $Pt^+$ (g) with $Bu^s$-SH**

The reaction of Au and Pt revealed the proton transfer product, $HL^+$, as the only major ion. Ions such as $MH_2S^+$ (eq. 6), $ML^+$ (eq. 1), $MH_2SL^+$, $ML_2^+$ (eq. 2) are observed with intensities less than 15%. $R^+$(eq. 31), $L^+$ (eq. 3) ions are observed at less than 4%. $MH_2SL^+$ is obviously the product of $MH_2S^+$ with L.

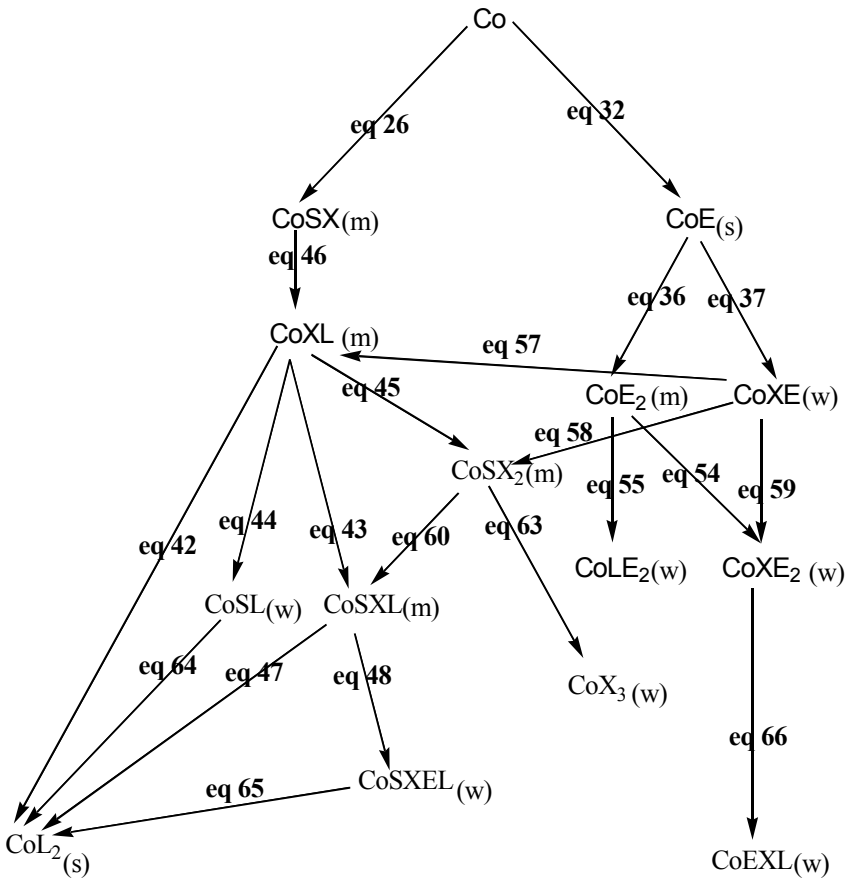


**Figure 10. Mechanistic pathways for the formation of products in the reactions of $Co^+$ with $Bu^s$ –SH.**

**TABLE 3**

**Times for the Complete Disappearance of the Metal Mono-Cations**

| Metal ion | Time |
|---|---|
| Ag | 3s |
| Zn, Pt | 4s |
| Fe, Co, Ni, Cu, Cr | 5s |
| Mn | 8s |
| Cd | 10s |
| Au | 40% remained after 60s |
| Pb | 31% remained after 150s |

## CONCLUSION

The production of metal ions by laser ablation of pure metal generally yields the mono-cation (Lubham, 1990; Cody *et al.*, 1980; Bucker & Freiser, 1989) which may not be a common ion observed in the condensed phase reactions. In general, the disappearance of the metal cation was observed to follow the pseudo-first order kinetics. The rate of the reaction depends on the nature of the metal ion. This is supported by the fact that different mechanistic pathways were adopted for the reactions of $Ni^+$, $Fe^+$ and $Co^+$.

Studying the reactivity is not a straightforward process. As mentioned previously, reactivity should be studied in terms of the time required for the initiation of the reaction, the time required for the complete disappearance of the metal ion as well as the variety of product ions obtained and, consequently, the reaction pathways followed.

In the case of complicated spectra, the presence of weak (or medium) intensity intermediate ions does not necessarily mean an insignificant reaction. On the contrary, it could be an indication of its high reactivity to yield other product ions. Such hypothesis requires further investigations that require the ability to isolate the ion to be studied and to observe its reactions separately. Under the conditions of these experiments, such process, especially for ions in low abundance, has proved to be extremely difficult.

Despite the different mechanisms presented, a number of reaction pathways patterns have been observed in common for a number of metals. In this respect:
- The reaction of $M^+$ to form $MX^+$ (eq. 4) and then $ML^+$ (eq. 8) has been observed for $Ag^+$, $Cu^+$, $Cd^+$, $Zn^+$ and $Ni^+$.
- Eq. 12, Eq. 17 and the sequences eq. 1 → eq. 2 →eq. 19 and eq. 1 → eq. 18 →eq. 20 are common for $Mn^+$ and $Cr^+$.
- Table 2 (2.2 & 2.3) shows a number of common pathways for $Ni^+$, $Fe^+$ and $Co^+$.

FT-ICR/MS ion molecule reaction studies provide a reliable technique for studying reaction mechanisms for simple reactions. In the case of the more complicated reactions, such as observed for $Ni^+$, $Fe^+$, and $Co^+$, the proposed mechanisms sometimes showed more than one route for the formation of one particular ion product. The intensity distribution of the different ions did not give enough information to positively indicate the correct mechanism.

Labelling the reactants could solve this uncertainty. Carrying out collision induced dissociation experiment could be another option. However, under the conditions of this experiment, one is unable to introduce more than one reactant (or collision gas) throughout the experiment.

Computational chemistry is simply the application of chemical, mathematical and computing skills to assist the understanding of chemical reactions of specific interests. With the rapid advances in computer hardware and software over the last decade, computational chemistry has become a useful method to investigate a chemical reaction by simulation and make predictions before running the actual experiments. Accordingly, computational chemistry constitutes the core for this current research with an attempt to resolve the above uncertainties.

## REFERENCES

Allison, R., Freas B. and Ridge, D.P. 1979. Cleavage of alkanes by transition metal ions in the gas phase. *J. Am. Chem. Soc*., 101: 1332-1333.

Buckner, S.W. and Freiser, B.S. 1989. *Gas phase inorganic chemistry*. D.H. Russell (Ed.), Press New York, pp. 279.

Choi, S.-S. and So, H.-Y. 2006. Proton transfer reactions and ion-molecule reactions of ionized $XCH_2CH_2Y$ (x and Y = OH or $NH_2$). *Bull. Korean Chem. Soc*., 27(4): 539-544.

Cody, R.B., Burnier, R.C., Reents Jr., W.D., Carlin, T.J., McCrery, D.A., Lengal, R.K. and Freiser, B.S. 1980. Laser ionization source for ion cyclotron resonance spectroscopy: Application to atomic metal in chemistry. *Int. J. of Mass Spectrom. and Ion Phys*., 33: 37.

Eller, K. and Schwarz, H. 1990. Trends across the periodic table – a screening of the gas-phase chemistry of d-block transition-metal ions with isocyanides. *Chem. Ber*., 123: 201-208 and references 1 therein.

Eller, K. and Schwarz, H. 1991. Organometallic chemistry in the gas phase. *Chem. Rev*., 91: 1121-1171.

Fisher, K.J. 2001. Gas-phase coordination chemistry of transition metal ions. *Progress in Inorganic Chemistry*, 50: 343- 432.

Greenwood, P.F., Strachan, M.G. Willett, G.D. and Wilson, M.A. 1990. Laser-induced molecular ion formation and gas-phase ion formation from polycyclic aromatic hydrocarbons, coals and coal products detected by Fourier transform mass spectrometry. *Org. Mass Spect*., 25: 353-362.

Kumar, M.R., Prabhakar, S., Reddy, T.J. and Vairamani, M. 2006. Generation of alkoxide anions from a series of aliphatic diols and alcohols and their ion-molecule reactions with carbon dioxide in the gas phase. *Eur. J. Mass Spectrom*., 12(1): 19-24.

Kumar, M.K., Sateesh, B., Prabhakar, S., Sastry, G.N. and Vairamani, M. 2006. Generation of regiospecific carbanions under electrospray ionization conditions and their selectivity in ion-molecule reactions with $CO_2$. *Rapid Commun. Mass Spectrom*., 20 (6): 987-993.

Lennon, J.D., Cole, S.P. and Glish, G.L. 2006. Ion/molecule reactions to chemically deconvolute the electrospray ionization mass spectra of synthetic polymers*, Anal. Chem*., 78(24): 8472-8476.

Lubham, D.M. 1990. *Lasers in mass spectrometry*. Oxford Univ. Press: New York.

El Nakat, J.H., Dance, I.G., Fisher, K.J., Rice, D. and Willett, G.D. 1991. Laser-ablation FTICR mass spectrometry of metal sulfides: gaseous anionic nickel-sulfur [$Ni_xS_y$] clusters. *J. Am Chem. Soc*.**,** 113: 5141-5148.

El-Nakat, J.H., Dance, I.G., Fisher, K.J. and Willet, G.D. 1992. Reactions of gaseous copper and silver ions, $Cu^+$, $Ag^+$, with thiols. *Polyhedron*, 11: 1125-1130.

El-Nakat, J.H., Dance, I.G., Fisher, K.J. and Willet, G.D. 1994. The reactions of $Zn^+$, $Cd^+$, $Hg^+$, and $Pb^+$ with benzene, substituted benzenes and thiols. *Polyhedron*, 13: 409-415.

Nguyen, T.H., Clezy, P.S., Willett, G.D., Paul, G.L., Tann, J. and Derrick, P.J. 1991. A laser desorption Fourier transform mass spectrometric study of dimethyl-8-acetyl-3,7,12,17-tetramethylporphyrin-2,18-dipropanoate. *Org. Mass Spect.,*, 26: 215-226.

Olesik, J.W. and Jones, D.R. 2006. Strategies to develop methods using ion-molecule reactions in a quadrupole reaction cell to overcome spectral overlaps in inductively coupled plasma mass spectrometry. *J. Anal. At. Spectrom*., 21(2): 141-159.

Xia, Y., Chrisman, P.A., Pitteri, S.J., Erickson, D.E. and McLuckey, S.A. 2006. Ion/molecule reactions of cation radicals formed from protonated polypeptides *via* gas-phase ion/ion electron transfer. *J. Am. Chem. Soc.*, 128(36): 11792-11798.

Zhang, R., Dinca, A., Fisher, K.J., Smith, D.R. and Willet, G.D. 2005. Gas-phase ion-molecule reactions of metal-carbide cations MCn+ (M = Y and La; n=2,4 and 6 with benzene and cyclohexane investigated by FTICR mass spectrometry and DFT calculations. *J. Phys. Chem. A*, 109(1): 157-164.